Earth and Planetary Science Letters 419 (2015) 125–133

Contents lists available at ScienceDirect

Earth and Planetary Science Letters

www.elsevier.com/locate/epsl

Are continental "adakites" derived from thickened or foundered lower crust?

Qiang Ma [a,b], Jian-Ping Zheng [b,*], Yi-Gang Xu [a,*], William L. Griffin [c], Rui-Sheng Zhang [b]

[a] State Key Laboratory of Isotope Geochemistry, Guangzhou Institute of Geochemistry, Chinese Academy of Sciences, Guangzhou 510640, China
[b] State Key Laboratory of Geological Processes and Mineral Resources, China University of Geosciences, Wuhan 430074, China
[c] ARC CoE for Core to Crust Fluid Systems/GEMOC, Macquarie University, NSW 2109, Australia

ARTICLE INFO

Article history:
Received 6 November 2014
Received in revised form 11 February 2015
Accepted 23 February 2015
Available online xxxx
Editor: A. Yin

Keywords:
continental "adakite"
source inheritance
North China Craton

ABSTRACT

The geochemical signatures of "adakites" are usually attributed to high-pressure (≥50 km) partial melting of mafic rocks, and accordingly the occurrence of adakitic magmas in continental settings is frequently used as an indicator of a thickened or foundered lower crust at the time of magma emplacement. These premises are built on experiments and modeling using an MORB-like source, but the probable source of continental "adakites" (i.e., continental lower crust) is compositionally different from MORB. To elucidate the effect of source inheritance and pressure on resultant melts, geochemical analyses and trace-element modeling have been carried out on Jurassic adakitic rocks from the northern part of the North China Craton. The results show that these continental adakitic melts can be generated at depths less than 40 km, and their "adakitic" signature is most likely inherited from their source rocks. Such conclusions can be applied to the Mesozoic adakitic magmas from the interior of the North China Craton. Only the "adakites" from collisional orogens (i.e., Tibet, Dabie UHP belt) require crustal melting at depths greater than 50 km, consistent with collision-induced crustal thickening in these areas. This study therefore highlights the importance of source composition when defining the formation conditions of magmatic rocks in general, and in particular questions the common use of "adakites" as an indicator of specific geodynamic situations.

© 2015 Elsevier B.V. All rights reserved.

1. Introduction

"Adakite" is used to describe a group of intermediate-felsic igneous rocks found in modern subduction zones; they are characterized by high Sr/Y (>40) and La/Yb (>20), depletion in Nb–Ta relative to light rare earth elements (LREEs) and large-ion lithophile elements (LILEs) and a lack of obvious Eu anomalies (Kay, 1978; Defant and Drummond, 1990). Melting experiments and modeling based on MORB-like basaltic source regions have shown that this adakitic geochemical signature can be achieved via high-pressure melting (≥1.5 GPa, Xiong et al., 2005; Nair and Chacko, 2008) of mafic rocks. In recent years, many igneous rocks with compositions similar to adakites have been identified in continental settings (Xu et al., 2002; He et al., 2011) and are inferred to be the products of similar high-pressure melting of mafic rocks. Thus, partial melting of thickened or foundered lower continental crust (LCC) at depths greater than 50 km is often invoked in the genesis of continental adakitic magmas (Chung et al., 2003; Gao et al., 2004). However, source composition, which is critical in the petrogenetic evaluation of magmatic rocks, has not been fully considered in these models. In particular, continental "adakites" tend to have radiogenic initial Sr and unradiogenic Nd isotopes (Fig. 1a), suggesting a source in ancient lower continental crust, which probably differs drastically in composition from MORB (Fig. 1b). More importantly, experiments have shown that adakitic melts can be produced by lower-pressure (10–12.5 kbar) melting of lower crust without leaving eclogitic residues (Qian and Hermann, 2013). It is therefore necessary to reassess the relative contributions of source inheritance *vs* high-P melting to the genesis of intra-continental adakitic melts.

To address this issue, we have carried out geochemical analyses and trace-element modeling on Jurassic adakitic volcanic rocks from the Yanshan belt in North China (Fig. 2), which have previously been interpreted as melts derived from a thickened lower crust (Zhang et al., 2008). We present a new petrogenetic model for continental adakitic rocks, in which the importance of source composition in the formation of "adakitic" magmas is emphasized.

* Corresponding authors.
E-mail addresses: jpzheng@cug.edu.cn (J.-P. Zheng), yigangxu@gig.ac.cn (Y.-G. Xu).

http://dx.doi.org/10.1016/j.epsl.2015.02.036
0012-821X/© 2015 Elsevier B.V. All rights reserved.

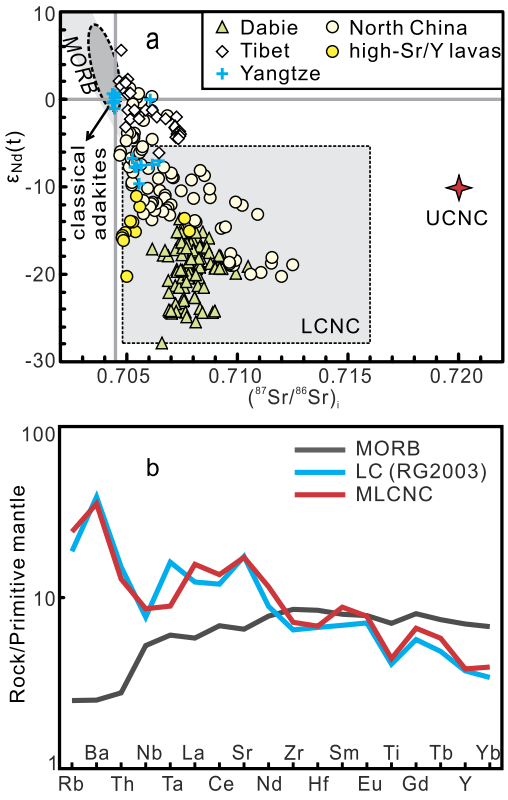

Fig. 1. (a) Sr–Nd isotopic compositions of Mesozoic–Cenozoic continental adakitic rocks from China. (b) Primitive mantle (PM) normalized trace-element patterns of mafic lower crust of the NCC (MLCNC), lower continental crust (RG2003) and MORB. Data sources: North China Craton, Gao et al. (2004), Yang and Li (2008), Ma et al. (2012), Chen et al. (2013), Xu et al. (2006) and this study; Yangtze Craton, Xu et al. (2002) and Wang et al. (2006a); Tibet Plateau, Chung et al. (2003), Hou et al. (2004) and Wang et al. (2005); Dabie Orogen, He et al. (2013) and references therein; lower continental crust, Rudnick and Gao (2003); MORB, Arevalo Jr. and McDonough (2010). Upper (UCNC) and lower crust (LCNC) of the North China after Jahn et al. (1999) and Jiang et al. (2013). Classical adakites, attributed to partial melting of subducted oceanic crust in modern arcs, are from the GeoRoc database (http://georoc.mpch-mainz.gwdg.de/georoc). Sr–Nd isotopes of MORBs (include both N-MORB and E-MORB) in (a) are from (http://www.earthchem.org/petdb). (For interpretation of the references to color in this figure legend, the reader is referred to the web version of this article.)

2. Geological background

The North China Craton (NCC; Fig. 2a) is well known worldwide for several reasons. It is one of the oldest (≥3.8 Ga, Liu et al., 1992) Archean cratons in the world. It has lost its lithospheric keel (>100 km) during the Phanerozoic, and represents the best example of craton-root destruction (Menzies et al., 1993; Griffin et al., 1998; Xu, 2001; Zheng et al., 2007). It is located between two major orogenic belts: the Qingling–Dabie–Sulu Orogenic belt to the south and the Central Asian Orogenic Belt to the north. The EW-trending Yanshan belt (Fig. 2a) is located in the northern part of the NCC. This region was tectonically dominated by post-collisional extensional regimes in the early Mesozoic, intraplate contractional environment in late Jurassic and crustal extension in early Cretaceous. Mesozoic terrestrial volcanic and clastic strata (Fig. S1, Supplementary online materials) unconformably overlie an Archean–Paleoproterozoic basement and Cambrian–Permian sedimentary units in this area. Volcanic rocks, varying from mafic to andesitic–felsic in composition, have been identified and interpreted as the results of cratonic destruction (Yang and Li, 2008; Ma et al., 2012). The middle-late Jurassic volcanic rocks across the Yanshan belt (Fig. 1b) mainly consist of intermediate-felsic lavas and pyroclastic rocks of the Haifanggou Formation (~173 Ma, this study; Fig. S2) and the overlying Lanqi Formation (166–153 Ma, Ma and Zheng, 2009).

3. Analytical methods

Geochemical data presented here include whole-rock compositions, Sr–Nd isotopes and zircon U–Pb and Hf isotopes; these are listed in Tables S1–S3. All the analyses were conducted at State Key Laboratory of Geological Processes and Mineral Resources, China University of Geosciences (Wuhan). Major- and trace-element compositions of whole rocks were measured by XRF and ICPMS, respectively. Sr and Nd isotopic ratios were analyzed using a Finnigan Triton TIMS. In-situ U–Pb and Hf isotope analyses of zircons were conducted by LA-ICPMS and MC-LA-ICPMS, respectively. Full details of the analytical methods are provided in Supplementary online materials.

4. Geochemistry

The samples collected range in composition from trachyandesite to rhyolite (Fig. 3a) with SiO_2 of 56.1–74.5 wt% and total alkalies ($Na_2O + K_2O$) of 5.7–9.7 wt%. These lavas show enrichment of LREEs over HREEs (Fig. 4a). They are enriched in LREEs, LILEs and Pb, with negative anomalies in high-field-strength elements (HFSEs) in the PM-normalized trace element plots. The lavas also have whole-rock Sr–Nd and zircon Hf isotopes (initial $^{87}Sr/^{86}Sr = 0.70434$ to 0.70787, $\varepsilon_{Nd}(t) = -20$ to -11, and $\varepsilon_{Hf}(t) = -21.7$ to $+4.1$; Tables S2–S3) indicative of derivation from older crustal rocks. Based on their compositions (Table S1), they can be subdivided into two groups (Figs. 3–5). Most of them, defined as high-Sr/Y lavas in this study, are characterized by high Sr (>540 ppm) and LREEs, low Y (8–21 ppm) and heavy rare earth elements (HREEs), a lack of obvious Eu anomalies (Fig. 4a), and low contents of MgO (<4.9 wt%), Ni (<41 ppm) and Cr (<57 ppm except 2 samples) (Fig. 3b); in all these features they are broadly similar to the high-silica adakites (Martin et al., 2005) and to experimental melts of mafic lower crust at 1–1.5 GPa (Qian and Hermann, 2013). The second group, defined as low-Sr/Y lavas, has higher Y (12–43 ppm) and HREEs and thus lower Sr/Y and La/Yb compared to the first group; it is similar to normal arc-related andesites, dacites and rhyolites (ADRs) (Fig. 5). The lavas of the second group also show enrichment in Th and U, lower Ba/Th and more variable Rb/Ba than the high-Sr/Y lavas, and have been interpreted as partial melts of upper lower-crustal to middle-crustal intermediate rocks (Yang and Li, 2008). This second group of rocks is not the focus of this study.

5. Petrogenesis of the Jurassic high-Sr/Y lavas

5.1. Assessing the role of AFC in petrogenesis of high-Sr/Y lavas

Crustal assimilation and/or fractional crystallization (AFC) can change the chemical and isotopic compositions of magmas and is considered as an important process in "adakite" petrogenesis (Castillo et al., 1999). However, the lack of correlation between initial Sr isotopic compositions and SiO_2 contents (Fig. S3) shows that crustal contamination or assimilation of intermediate-felsic crustal rocks is not appreciable in most of the investigated lavas. Using an adakitic dacite (C4-4-88) from a modern arc (Defant et al., 1992) as representative of "adakites" before continental crust assimilation, the modeled Sr–Nd isotopes of melts resulting from contamination are dramatically different from those of the Jurassic high-Sr/Y lavas (Fig. S3), which also suggests their Sr–Nd isotopes are not the product of crustal interaction. Moreover, AFC modeling on the representative lavas (Supplementary online materials) suggests that AFC processes would drive the

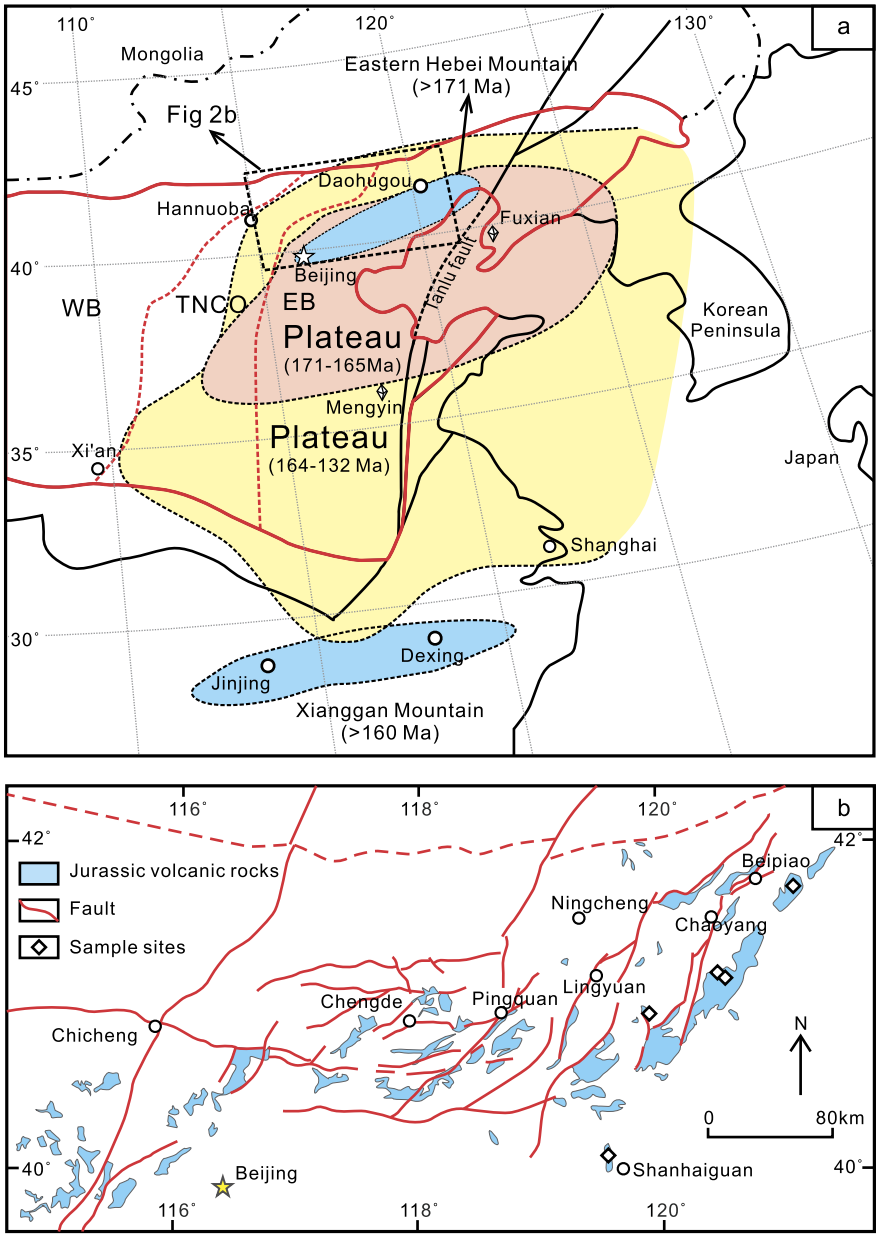

Fig. 2. (a) Simplified geological maps showing distributions of the hypothetical Jurassic–Cretaceous plateau in eastern China (Zhang et al., 2008) and (b) the Jurassic volcanic rocks in the Yanshan belt.

magmas toward low Sr/Y and negative Eu anomalies (Fig. S4), which is the opposite of their adakitic signatures. Although it is difficult to rule out processes such as the assimilation of mafic crust and recharge–evacuation–fractional crystallization (REFC; Lee et al., 2014), several lines of evidence suggest that these processes would only have played a limited role in generating their high Sr/Y adakitic geochemical signature. 1) Sr/Y ratios of mafic lower crustal rocks beneath the NCC are significantly lower than those of Mezozoic high-Sr/Y lavas in Yanshan belt (Fig. 5). 2) Invariant or slight decreasing Sr/Y with decreasing MgO (Fig. S5) suggests that the high Sr/Y geochemistry cannot be attributed to REFC processes (nor to AFC). 3) Modeling of the compositional evolution of the high-Sr/Y lavas undergoing REFC (Fig. S5; Lee et al., 2014) suggests that REFC processes are possible but did not produce adakitic geochemistry. In summary, AFC or REFC processes could only have played a limited role, at least without substantially affecting the adakitic geochemistry, during their evolution.

5.2. Origin of the adakitic geochemical signature

"Adakite" was originally proposed as a term to describe intermediate-felsic igneous rocks that are derived from melting of subducted oceanic slabs (Defant and Drummond, 1990). Currently, the term "adakite" is used for a wide variety of igneous rocks, whose sole common feature is high Sr/Y and La/Yb ratios (Moyen, 2009). This loose geochemical definition may not be an appropriate petrological term; it causes confusion in understanding the petrogenesis of many igneous rocks. We argue that the term *adakite* cannot be used in many cases, and should be replaced by "adakites", adakitic rocks or something with "adakitic" signatures. Various models have been proposed to account for the origin of intermediate-felsic igneous rocks with "adakitic" signatures (Martin et al., 2005; Castillo, 2012). The Jurassic high-Sr/Y lavas in the NCC have higher K_2O contents (≥1.5 wt%) and K_2O/Na_2O (≥0.5), and more radiogenic Sr and less radiogenic Nd isotopes than classical adakites (Fig. 1a), making it unlikely that they were generated from sub-

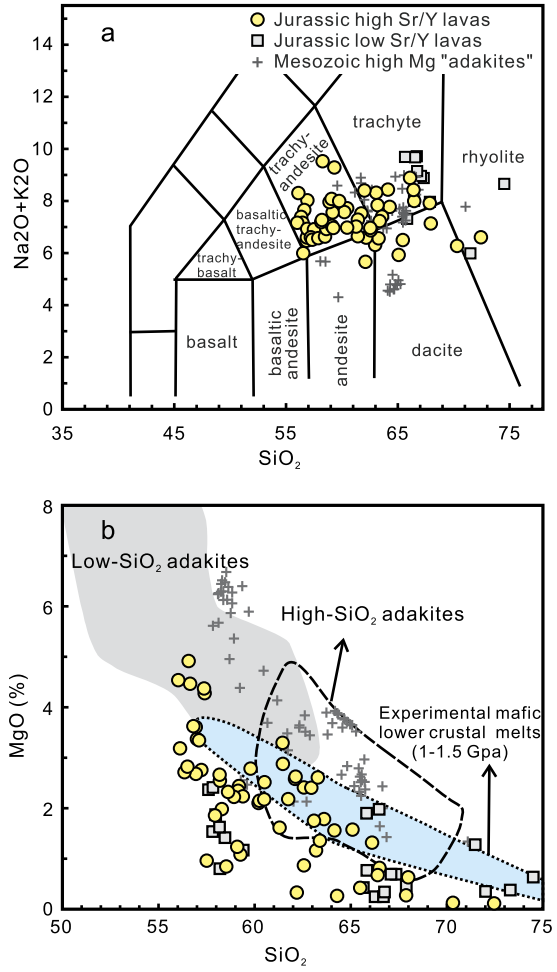

Fig. 3. Plots of (a) $Na_2O + K_2O$ vs SiO_2 and (b) MgO vs SiO_2 for Jurassic lavas in the Yanshan Belt, North China. Data for Mesozoic lavas in the Yanshan belt are from Gao et al. (2004), Wang et al. (2006b), Yang and Li (2008), Ma et al. (2012) and this study; fields of high-SiO_2 adakites and low-SiO_2 adakites are from Martin et al. (2005); data for experimental melts from mafic lower crustal (1–1.5 GPa) are from Qian and Hermann (2013).

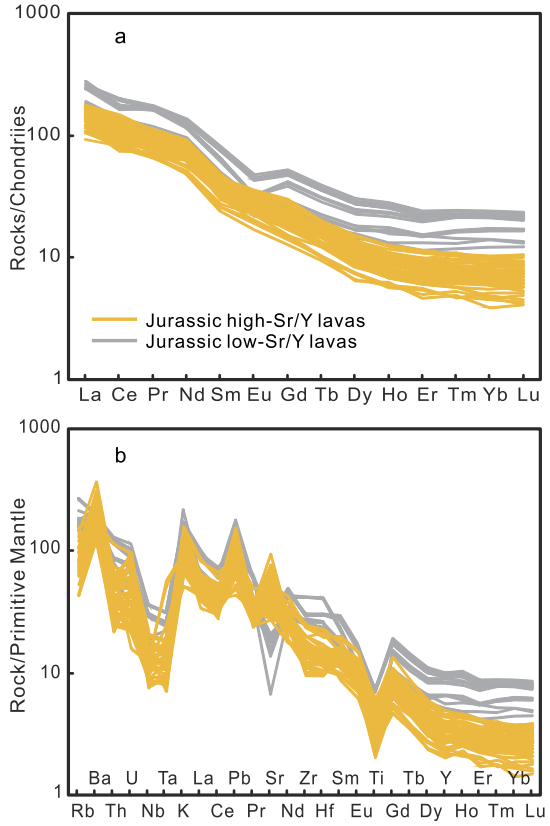

Fig. 4. Chondrite-normalized REE patterns (a) and primitive mantle-normalized trace-element patterns (b) for Jurassic lavas in the Yanshan Belt, North China. Normalizing values are from McDonough and Sun (1995).

ducted basalts (Castillo, 2012). As discussed above, AFC processes involving a basaltic magma can also be ruled out. The studied rocks typically have moderate SiO_2 contents (mostly <70%), low Rb/Ba (<0.1), Nb/U (mostly <17), Ce/Pb (<10), and old Nd–Hf model ages (~2.5 Ga), consistent with a derivation from an ancient mafic lower crust. Such adakitic rocks are commonly considered as products of melting of a thickened or foundered mafic LCC (Gao et al., 2004; Zhang et al., 2008). However, a serious problem with this interpretation is that the ancient mafic LCC inferred for the source of the Jurassic continental adakitic rocks is different from MORB (Fig. 6).

A series of partial-melting models was designed to elucidate the effect of source inheritance and melting pressure on the origin of these continental adakitic rocks. The modeling for selected incompatible trace elements was based on equilibrium melting and using the modal batch-melting equation (Shaw, 1970). The assumed source (Table 1) is the mafic lower crust of the North China Craton (MLCNC), which is represented by the weighted average of Archean mafic granulite terrains (Jahn and Zhang, 1984; Liu et al., 1999; Zhai et al., 2001) and mafic lower crustal xenoliths in Phanerozoic basalts and kimberlites (Liu et al., 2001; Zheng et al., 2004). Given the wide compositional range of mafic lower crust in the NCC, end-members represented by two granulites based on their SiO_2 contents (Fig. 6) were also taken as alternative sources. Since modeling results involving the average composition capture the first-order behavior of the magmatic system, those using average MLCNC are emphasized in the following discussion. P–T conditions for these lower-crustal samples have been previously estimated using cation-exchange thermobarometers. They record peak equilibrium temperatures from 745 to 950 °C and pressures from 7 to 14 kbar (Liu et al., 2001 and references therein; Zhai et al., 2001; Zheng et al., 2004), equivalent to a depth of 23 to 46 km. Different models have been proposed to account for the origin of the precursors of these granulite-facies samples, including solidified basaltic melts either in arc environments or mantle plumes and subduction erosion (Goss and Kay, 2006; Zhai et al., 2001; Zheng et al., 2012), Phanerozoic basaltic underplating (Liu et al., 2001) and residues after anatexis (Jiang et al., 2013). These lower-crustal samples display a wide range in SiO_2 (43 to 54 wt%), Al_2O_3 (3.8 to 24.4 wt%), MgO (3.4 to 18.6 wt%), CaO (4.5 to 21.7 wt%) and Mg# (40 to 86) (Fig. 6). Their weighted average major-element compositions are similar to the lower crust composition given by Rudnick and Gao (2003) and the starting material of melting experiments by Qian and Hermann (2013). Although they show a variety of REE distributions, the average compositions of both granulite terrains and xenoliths have light REE enriched patterns (Fig. 6d), which are dramatically different from MORB. The MLCNC is also very similar in terms of trace elements to the lower crustal composition given by Rudnick and Gao (2003) (Fig. 1b), but has higher Nb/Ta (17.1) than RG2003 (8.3). The high Nb/Ta nature of the lower crust of the NCC was also suggested by Gao et al. (1998) and Liu et al. (1999).

The partition coefficients used in the calculations (Table 1) are from intermediate-felsic magmas and experimental runs under equilibrium conditions that would produce melting of the continental lower crust. Three different melting depths, i.e., ≤33 km,

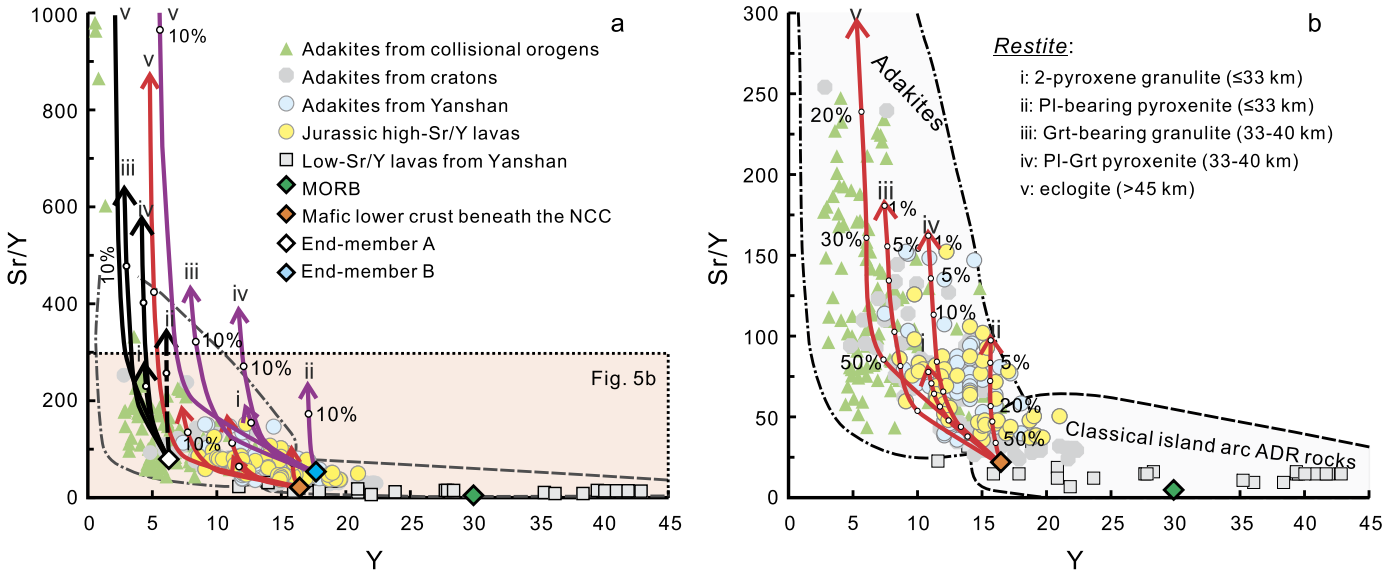

Fig. 5. Plot of Sr/Y vs Y for the Mesozoic andesitic–felsic volcanic rocks in the Yanshan belt, North China. Partial-melting curves are calculated for batch melting of the mafic lower crust of the NCC (MLCNC with Y = 16.5 ppm and Sr/Y = 21), End-member A (Grt-bearing granulite with Y = 6.35 ppm and Sr/Y = 75) and End-member B (2-pyroxene granulite with Y = 17.8 ppm and Sr/Y = 50) with melt fractions of 1%, 5%, 10%, 20%, 30% and 50% (white circles on each of the model curves). Fields of adakites and classical island andesite–dacite–rhyolite (ADR) rocks are modified from Defant and Drummond (1990). (For interpretation of the references to color in this figure legend, the reader is referred to the web version of this article.)

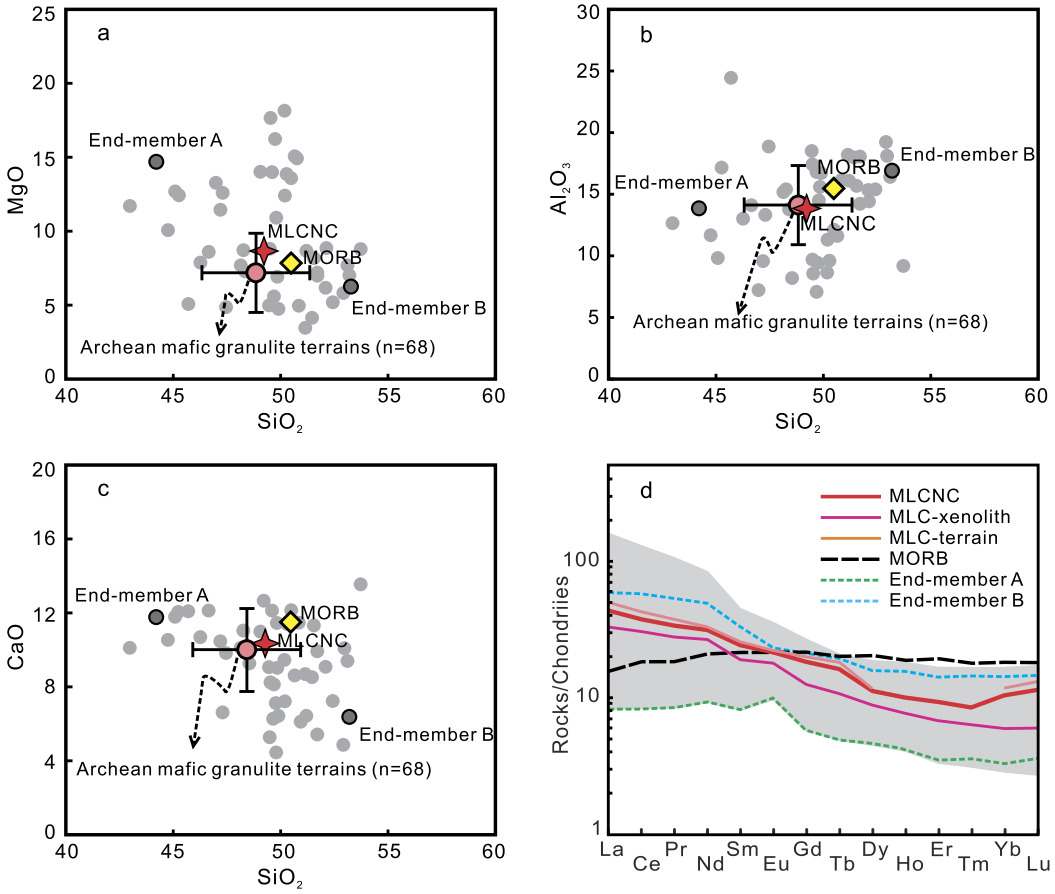

Fig. 6. Plots of (a) MgO, (b) Al_2O_3 and (c) CaO vs SiO_2 and (d) Chondrite-normalized REE patterns for lower-crustal samples from NCC. Data source: lower-crustal samples marked as grey circles are from Jahn and Zhang (1984), Liu et al. (2001) and Zheng et al. (2004); Archean mafic granulite terrains ($n = 68$) marked as pink circle with error bar (1σ) are from Liu et al. (1999) and Zhai et al. (2001) which did not report the composition of individual samples; MORB are from Arevalo Jr. and McDonough (2010). (For interpretation of the references to color in this figure legend, the reader is referred to the web version of this article.)

Table 1
Partition coefficients and assumed source rocks for trace elemental modeling. Data source: D for Opx, Grt and Am from Qian and Hermann (2013); D for Cpx and Pl from Severs et al. (2009); $D_{Nb, Ta, Zr, Hf}$ for Rt from Xiong et al. (2005); $D_{Nb, Ta}$ for Ilm from Nehring et al. (2010); Values not given by above literature are compiled from Bédard (2006). Cpx, clinopyroxene; Opx, orthopyroxene; Pl, plagioclase; Grt, garnet; Am, amphibole; Rt, rutile; Ilm, ilmenite.

Element	Presumed source	Partition coefficients						
	MLCNC	Cpx	Opx	Pl	Grt	Am	Rt	Ilm
Rb	16.9	0.010	0.008	0.068	0.0007	0.045	0.0076	0.025
Ba	315	0.001	0.013	0.186	0.002	0.144	0.0043	0.018
Th	1.02	0.104	0.013	0.095	0.0075	0.011	0.20	0.09
Nb	5.99	0.008	0.057	0.008	0.015	0.339	94	10.17
Ta	0.35	0.028	0.04	0.053	0.044	0.239	129	11.95
La	11.1	0.082	0.022	0.088	0.005	0.089	0.0057	0.015
Ce	24.5	0.059	0.038	0.339	0.014	0.184	0.0065	0.012
Sr	346	0.101	0.033	2.422	0.005	0.358	0.036	0.0022
Nd	14.5	0.38	0.114	0.054	0.137	0.514	0.0082	0.01
Zr	76.0	0.097	0.082	0.005	0.656	0.187	5.0	2.3
Hf	1.91	0.171	0.166	0.016	0.384	0.311	7.1	2.4
Sm	3.58	0.259	0.241	0.033	0.862	0.966	0.0954	0.009
Eu	1.20	0.626	0.16	0.397	0.896	0.811	0.00037	0.01
Ti	5194	0.473	1.409	0.043	1.223	3.094	45	12.5
Gd	3.62	0.907	0.437	0.037	3.149	1.718	0.0106	0.011
Tb	0.58	0.763	0.5725	0.025	5.425	2.2885	0.0111	0.018
Y	16.5	0.949	0.743	0.012	9.532	3.156	0.0118	0.037
Yb	1.74	0.973	1.097	0.01	11.697	3.786	0.0126	0.13

33–40 km and >45 km, were considered, corresponding to different residual mineral assemblages defined by melting experiments (Qian and Hermann, 2013). Pyroxene-rich, rather than amphibole-rich, residue during lower continental crustal melting are considered, because representative lower-crustal rocks from the NCC only contain rare hydrous phases. Moreover, many magmas with adakitic signatures in arcs are also supposed to be in equilibrium with lower crustal pyroxenites (e.g. Lee et al., 2007). We tested the effects of different weight fractions of other minerals in the restite at given proportions of clinopyroxene and orthopyroxene. Representative partial-melting residues are as following: 1) two-pyroxene granulite (Cpx:Opx:Am:Pl:Ilm = 40:20:29:10:1) and Pl-bearing pyroxenite (Cpx:Opx:Am:Pl:Ilm = 60:25:9:5:1) at ≤33 km, 2) Grt-bearing granulite (Cpx:Opx:Am:Grt:Pl:Ilm:Rt = 40:20:24:10:5:0.5:0.5) and Pl–Grt pyroxenite (Cpx:Opx:Grt:Pl:Ilm = 60:25:8:5:2) at 33–40 km, and 3) eclogite (Cpx:Grt:Rt = 70:29:1) at >45 km. In general, rutile mode decreases during melting (Pertermann and Hirschmann, 2003) and it disappears at degree of melting greater than 40% (Qian and Hermann, 2013).

The results of these calculations, including trace-element concentrations and ratios, and a statistical assessment of the differences between the model results and target melt values, are summarized in Table S5. For comparison, trace-element modeling on melts derived from an MORB-like source under the same conditions is also presented in Table S6. Our modeling results are further compared with previous experiments and modeling using similar sources and P–T conditions (Table S6). Our results closely match the experimental and modeled melts from the lower crust of RG2003 (Qian and Hermann, 2013) at 10–13.5 kbar. Because the partition coefficients of Y and HREE between garnet and melt used in this study (e.g. $D_Y^{Grt/melt} = 9.532$) are lower than those calculated by Qian and Hermann (2013) (e.g. $D_Y^{Grt/melt} =$ 14.608 to 16.141 at 15 kbar), the Sr/Y and La/Yb ratios of modeled melts at high pressure (depth >45 km) are considerably lower than those from the experimental melts produced under similar conditions.

The results suggest that melts in equilibrium with eclogitic residues (depths >45 km) from the MLCNC would be more deficient in HREE and Y, and higher in Sr/Y than the Jurassic high-Sr/Y lavas in the Yanshan belt (Figs. 5, 7 and 8). At lower pressures, with granulites or pyroxenites as residues from the MLCNC source, the modeled trace-element compositions of the melts become similar to those of the Mesozoic high-Sr/Y lavas of the NCC. For example, 5–30% partial melting of the MLCNC, leaving a residue without garnet, produces melts that have high Sr and LREE, low Y and HREE, thus high Sr/Y ratios. When minor garnet (<10%) is present in the residues, the resultant melts also have an adakitic composition, with higher Sr/Y and lower HREE contents than the melts in equilibrium with two-pyroxene granulites. Although the modeled melts produced by 10–40% melting of MLCNC at depths less than 40 km are generally consistent with natural Jurassic high-Sr/Y lavas (Figs. 7–8), there are still some differences. The higher Nb and Zr contents of the low-degree melts reflect an underestimate of accessory minerals in the residue, e.g. Ti-oxide phases and zircon. The contents of highly incompatible elements such as Rb, Ba in the modeled melts overlap with the ranges of the NCC high-Sr/Y lavas but are systematically higher than their mean and median values at <20 wt% melting. This can be attributed to the low melt fraction and overestimation of the source compositions (lower crustal xenoliths in Hannuoba basalts have markedly high Rb and Ba; Liu et al., 2001). However, such differences between the model results and the target melts do not affect the use of trace-element patterns or ratios (Table S5 and Figs. 7–8) to explain the generation of melts with the adakitic signature.

The negative Nb–Ta anomaly associated with high Nb/Ta ratios in adakitic rocks and TTGs is an important fingerprint of the involvement of rutile in magma genesis (Foley et al., 2002), and has been proposed as an indicator of high-pressure melting regimes (≥1.5 GPa) when an MORB-like source is assumed (Xiong et al., 2005). This hypothesis may not apply to the LCC-derived adakitic melts, because of the intrinsic depletion of Nb–Ta in their source (Rudnick and Gao, 2003) and rutile can be stable at P ≥ 1.0 GPa in the lower continental crust (Qian and Hermann, 2013). Our modeling also suggests that rutile is not a necessary residual phase during the generation of the late Mesozoic high Sr/Y lavas (Figs. 7–8). This is further supported by the similarity of Nb/Ta ratios in the Jurassic high-Sr/Y lavas (~17.5) and in the lower crust beneath eastern China (~17.9, Gao et al., 1998). The negative Nb–Ta anomaly can simply be attributed to source characteristics and the involvement of other Ti-oxide phases, such as ilmenite and sphene, in melting or crystal fractionation.

High Sr concentrations and the absence of an Eu anomaly in adakitic rocks are commonly interpreted as indicative of a plagioclase-free residue. However, Sr enrichment occurs in melts in equilibrium with a mafic LCC source with <20% plagioclase (Qian and Hermann, 2013). It also has been shown that D_{REE} of plagio-

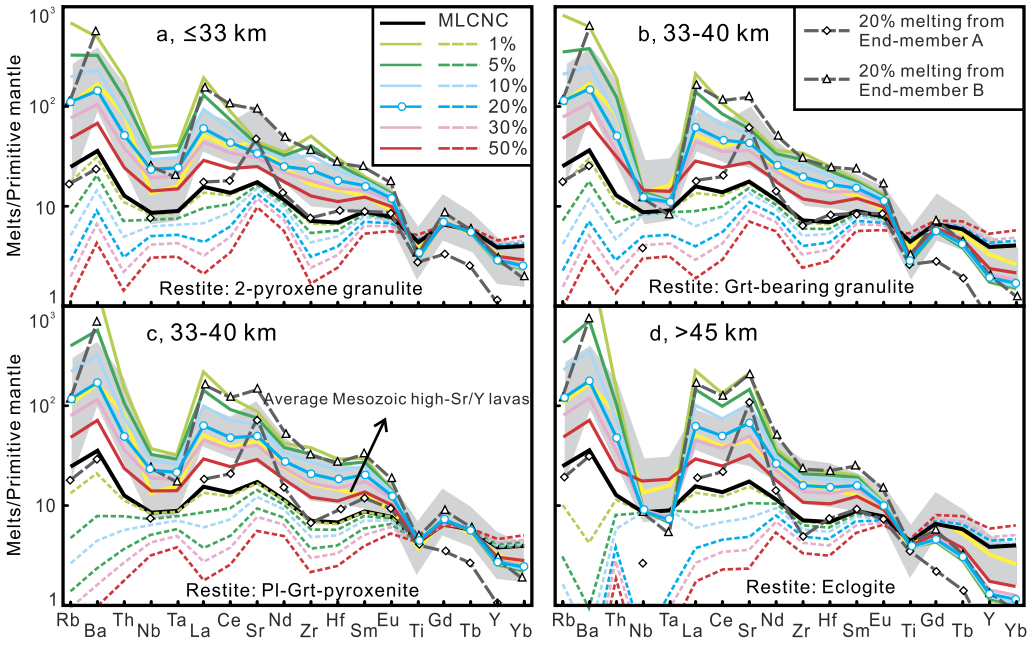

Fig. 7. Primitive-mantle-normalized trace-element patterns of modeled partial melts (solid lines) and restites (dash lines) of mafic lower crust in the NCC. Assumed mineral assemblages of the restites are the same as in Fig. 5. The shaded region is the field of Mesozoic adakitic lavas in the Yanshan belt. Melts derived from 20% batch melting of end members are also shown. Trace-element patterns of the modeled melts produced by low-degree melting of End-member B are generally consistent with those from the melting of average MLCNC. Melts derived from End-member A (a Grt-bearing granulite) at all P–T conditions have considerably lower HREE than those of target lavas and melts from average MLCNC. This suggests that such Grt-bearing granulite are not appropriate source rocks. (For interpretation of the references to color in this figure legend, the reader is referred to the web version of this article.)

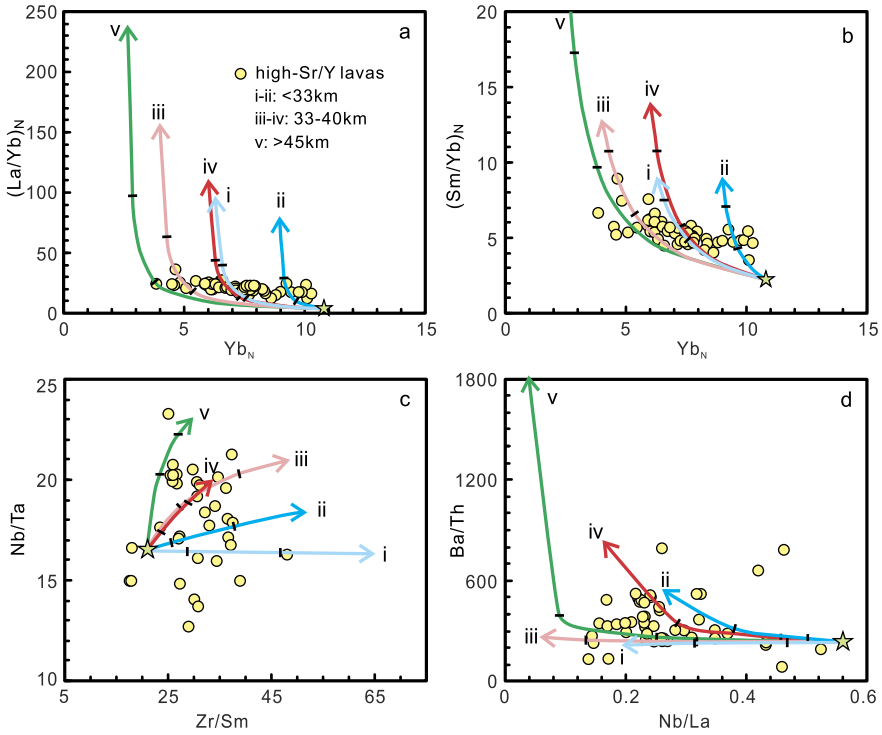

Fig. 8. Plots of (a) $(La/Yb)_N$ vs Yb_N, (b) $(Sm/Yb)_N$ vs Yb_N, (c) Nb/Ta vs Zr/Sm and (d) Ba/Th vs Nb/La for modeled melts from partial melting of mafic lower crust of the NCC. i) two-pyroxene granulite at ≤33 km; ii) Pl-bearing pyroxenite at ≤33 km; iii) Grt-bearing granulite at 33–40 km; iv) Pl-Grt pyroxenite at 33–40 km; v) eclogite at >45 km. Short lines on each of the model curves represent melt fractions at 10% and 40%. Note: the modeled melts presented here do not consider that the rutile mode decreases during melting.

clase decreases with increasing anorthite content (Bédard, 2006). The residual plagioclase has an anorthite content with An_{50-77} as shown by melting experiments on mafic lower-crustal compositions (Qian and Hermann, 2013). The partition coefficient for Eu between Ca-rich plagioclase and felsic melt is about 0.4 (Severs et al., 2009), indicating that the presence of Ca-rich plagioclase cannot effectively generate negative Eu anomalies during fractionation and/or partial melting. This is supported by our mod-

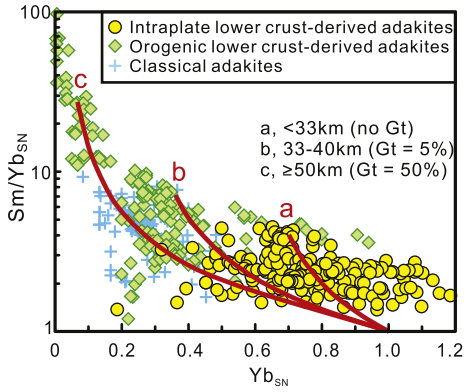

Fig. 9. $(Sm/Yb)_{SN}$ vs Yb_{SN} diagram for adakitic rocks derived from the lower crust. The curves represent models for the partial melting of mafic rocks with restites of (a) 2-Pyroxene Granulite without garnet, (b) Garnet-bearing Granulite with 5% garnet, and (c) Eclogite with 50% garnet. Intraplate "adakites" are represented by the Mesozoic continental adakitic rocks in the Yangtze and North China Cratons; orogenic "adakites" are from the Central Andes (Goss and Kay, 2009) and continental adakitic rocks from the Tibetan Plateau and the Dabie Orogen. Data sources are the same as in Fig. 1 except for adakitic rocks from Dabie Orogen (He et al., 2011 and references therein). Subscript SN denotes source-normalized data, where the compositions of the assumed sources are MORB with Yb = 3 ppm and Sm/Yb = 1.08 for classical adakites and those from the Central Andes, and the mafic lower continental crust with Yb = 1.5 ppm and Sm/Yb = 1.87 for continental adakitic rocks.

eling, which shows that melts from the mafic lower crust of the NCC display negligible or even positive Eu anomalies when minor plagioclase is present in the restite (Fig. 7).

The modeling presented here strongly suggests that the main compositional characteristics of the late Mesozoic adakitic rocks in the NCC (e.g. high Sr/Y, Nb–Ta depletion, and lack of Eu anomaly) are inherited from their source rocks, rather than reflecting melting at high pressure (≥1.5 GPa). High-Sr/Y lavas with high MgO and variable zircon Hf isotopes in some of the Lanqi Formation (Fig. S2) can be attributed to the involvement of minor mantle-derived magmas in their source (Ma et al., 2012) or magma chamber (Chen et al., 2013). Basaltic underplating at the base of the lower crust beneath the NCC during late Mesozoic time has been recognized by studies of contemporary basalts (Yang and Li, 2008) and xenoliths in Cenozoic basalts (Zhang et al., 2013). We therefore propose that the Jurassic high-Sr/Y lavas from the NCC were generated by partial melting of an ancient mafic lower continental crust, with heat provided by continuous magmatic underplating.

6. Geodynamic implications

6.1. Destruction of the North China Craton

Continental adakitic rocks are widely used as a geodynamic indicator of crustal thickening, orogenic collapse and lithospheric delamination (e.g. Chung et al., 2003). This interpretation and the widespread occurrence of Mesozoic adakitic rocks in the NCC have led to suggestions of the presence of a paleo-plateau in the eastern NCC during late Mesozoic time (Fig. 2a; Zhang et al., 2008); by inference this model involves delamination of the lower crust (Gao et al., 2004). The potential problems associated with this foundering hypothesis have been laid out by Lee (2014). The main weakness of this hypothesis is that the effect of source composition on adakitic chemistry is not taken into account. As discussed above, the formation of such "adakitic" melts is controlled by the composition of the melting lower crust, and as a consequence, interpretations of "adakitic" rocks as markers of deep melting are far from robust. Trace-element modeling suggests that the melting depth required to produce the Mesozoic "adakitic" rocks in the Yanshan belt is from ≤33 to 40 km (Figs. 5, 7 and 8). This is similar to the thickness of the normal continental crust, which argues against a role for a thickened plateau-type crust, or its delamination, in the generation of the continental "adakites". Other evidence supporting this argument include analyses of paleo-drainage systems and the presence of Jurassic terrestrial fossils (plants, insects and vertebrates) that indicate a low-elevation, warm and humid environment (Jiang et al., 2008; Li et al., 2013).

6.2. Adakitic rocks in intraplate and orogenic settings

Crustal thickening rarely occurs in an intraplate setting, but may be common in an orogenic setting. Deep-seated adakitic rocks (derived from >50 km depth) are therefore expected to occur in orogenic settings. We have compared the intraplate and orogenic adakitic rocks in an $(Sm/Yb)_{SN}$ vs Yb_{SN} diagram (Fig. 9). It is clear that continental "adakites" from collisional orogens generally have high $(Sm/Yb)_{SN}$ and low Yb_{SN}, similar to adakitic magma from modern convergent margins and to modeled melts in equilibrium with a garnet-rich residue. In contrast, continental "adakites" from ancient cratons that lack other evidence for a thickened lower crust have systematically lower $(Sm/Yb)_{SN}$ and higher Yb_{SN}, similar to our modeled melts in equilibrium with a residue containing little or no garnet (<10%). Consequently, the different REE budgets between adakitic rocks from cratonic areas (excluding those formed prior to cratonization) and collisional orogens can be attributed to the effects of source inheritance and high-pressure melting, respectively.

7. Concluding remarks

Variations in source composition have a profound influence on the origin of high Sr/Y "adakitic" melts in a continental setting. The case of the NCC demonstrates that the generation of "adakitic" magmas in intracontinental settings may not require a thickened or foundered lower crust. Rather they can be produced at relatively low pressures, and their peculiar compositions are inherited from their source rocks during partial melting. The role of source composition should be taken into consideration while dealing with the petrogenesis of adakitic and TTG magmas.

Acknowledgements

We thank Dr. A. Yin (journal editor) and Drs. C.T. Lee, P. Castillo, A. Hastie, H. Rollinson and an anonymous reviewer for their constructive comments and suggestions on different versions of the manuscript. This work was supported by the NSFC (41130315, 91214204 and 91014007). This is publication 2046 from GIG-CAS, 607 from the ARC Centre of Excellence for Core to Crust Fluid Systems, and 996 from GEMOC.

Appendix A. Supplementary material

Supplementary material related to this article can be found online at http://dx.doi.org/10.1016/j.epsl.2015.02.036.

References

Arevalo Jr., R., McDonough, W.F., 2010. Chemical variations and regional diversity observed in MORB. Chem. Geol. 271, 70–85.
Bédard, J.H., 2006. Trace element partitioning in plagioclase feldspar. Geochim. Cosmochim. Acta 70, 3717–3742.
Castillo, P.R., Janney, P.E., Solidum, R.U., 1999. Petrology and geochemistry of Camiguin Island, southern Philippines: insights to the source of adakites and other lavas in a complex arc setting. Contrib. Mineral. Petrol. 134, 33–51.
Castillo, P.R., 2012. Adakite petrogenesis. Lithos 134–135, 304–316.

Chen, B., Jahn, B., Suzuki, K., 2013. Petrological and Nd–Sr–Os isotopic constraints on the origin of high-Mg adakitic rocks from the North China Craton: tectonic implications. Geology 41, 91–94.
Chung, S.L., Liu, D.Y., Ji, J.Q., Chu, M.F., Lee, H.Y., Wen, D.J., Lo, C.H., Lee, T.Y., Qian, Q., Zhang, Q., 2003. Adakites from continental collision zones: melting of thickened lower crust beneath southern Tibet. Geology 31, 1021–1024.
Defant, M.J., Drummond, M.S., 1990. Derivation of some modern arc magmas by melting of young subducted lithosphere. Nature 347, 662–665.
Defant, M.J., Jackson, T.E., Drummond, M.S., De Boer, J.Z., Bellon, H., Feigenson, M.D., Maury, R.C., Stewart, R.H., Cawood, A.P., 1992. The geochemistry of young volcanism throughout western Panama and southeastern Costa Rica: an overview. J. Geol. Soc. Lond. 149, 569–579.
Foley, S., Tiepolo, M., Vannucci, R., 2002. Growth of early continental crust controlled by melting of amphibolite in subduction zones. Nature 417, 837–840.
Gao, S., Luo, T.C., Zhang, B.R., Zhang, H.F., Han, Y.W., Zhao, Z.D., Hu, Y.K., 1998. Chemical composition of the continental crust as revealed by studies in East China. Geochim. Cosmochim. Acta 62, 1959–1975.
Gao, S., Rudnick, R.L., Yuan, H.L., Liu, X.M., Liu, Y.S., Xu, W.L., Ling, W.L., Ayers, J., Wang, X.C., Wang, Q.H., 2004. Recycling lower continental crust in the North China craton. Nature 432, 892–897.
Goss, A.R., Kay, S.M., 2006. Steep REE patterns and enriched Pb isotopes in southern Central American arc magmas: evidence for forearc subduction erosion? Geochem. Geophys. Geosyst. 7, Q05016. http://dx.doi.org/10.1029/2005GC001163.
Goss, A.R., Kay, S.M., 2009. Extreme high field strength element (HFSE) depletion and near-chondritic Nb/Ta ratios in Central Andean adakite-like lavas (~28°S, ~68°W). Earth Planet. Sci. Lett. 279, 97–109.
Griffin, W.L., Zhang, A., O'Reilly, S.Y., Ryan, C.G., 1998. Phanerozoic evolution of the lithosphere beneath the Sino-Korean craton. In: Flower, M., Chung, S.L., Lo, C.H., Lee, T.Y. (Eds.), Mantle Dynamics and Plate Interactions in East Asia, vol. 27. American Geophysical Union, Washington, DC, pp. 107–126.
He, Y., Li, S., Hoefs, J., Huang, F., Liu, S., Hou, Z., 2011. Post-collisional granitoids from the Dabie orogen: new evidence for partial melting of a thickened continental crust. Geochim. Cosmochim. Acta 75, 3815–3838.
He, Y., Li, S., Hoefs, J., Kleinhanns, I.C., 2013. Sr–Nd–Pb isotopic compositions of Early Cretaceous granitoids from the Dabie orogen: constraints on the recycled lower continental crust. Lithos 156–159, 204–217.
Hou, Z.Q., Gao, Y.F., Qu, X.M., Rui, Z.Y., Mo, X.X., 2004. Origin of adakitic intrusives generated during mid-Miocene east–west extension in southern Tibet. Earth Planet. Sci. Lett. 220, 139–155.
Jahn, B.M., Zhang, Z.Q., 1984. Archean granulite gneisses from eastern Hebei Province, China: rare earth geochemistry and tectonic implications. Contrib. Mineral. Petrol. 85, 224–243.
Jahn, B.M., Wu, F.Y., Lo, C.H., Tsai, C.H., 1999. Crust-mantle interaction induced by deep subduction of the continental crust: geochemical and Sr–Nd isotopic evidence from post-collisional mafic–ultramafic intrusions of the northern Dabie complex, central China. Chem. Geol. 157, 119–146.
Jiang, H., Ferguson, D.K., Li, C., Cheng, Y., 2008. Fossil coniferous wood from the Middle Jurassic of Liaoning Province, China. Rev. Palaeobot. Palynol. 150, 37–47.
Jiang, N., Guo, J., Chang, G., 2013. Nature and evolution of the lower crust in the eastern North China craton: a review. Earth-Sci. Rev. 122, 1–9.
Kay, R.W., 1978. Aleutian magnesian andesites: melts from subducted Pacific ocean crust. J. Volcanol. Geotherm. Res. 4 (1–2), 117–132.
Lee, C.T.A., Morton, D.M., Kistler, R.W., Baird, A.K., 2007. Petrology and tectonics of Phanerozoic continent formation: from island arcs to accretion and continental arc magmatism. Earth Planet. Sci. Lett. 263, 370–387.
Lee, C.T.A., 2014. Physics and chemistry of deep continental crust recycling. In: Holland, H.D., Turekian, K.K. (Eds.), Treatise on Geochemistry, second edition. Elsevier, Oxford, pp. 423–456.
Lee, C.A., Lee, T.C., Wu, C., 2014. Modeling the compositional evolution of recharging, evacuating, and fractionating (REFC) magma chambers: implications for differentiation of arc magmas. Geochim. Cosmochim. Acta 143, 8–22.
Li, H., Xu, Y., Liu, Y., Huang, X., He, B., 2013. Detrital zircons reveal no Jurassic plateau in the eastern North China Craton. Gondwana Res. 24, 622–634.
Liu, D.Y., Nutman, A.P., Compston, W., Wu, J.S., Shen, Q.H., 1992. Remnants of ≥3800 Ma crust in the Chinese part of the Sino-Korean craton. Geology 20, 339–342.
Liu, Y.S., Gao, S., Luo, T.C., 1999. Geochemistry of granulites in North China craton: implications for the composition of Archean lower crust. Geol. Geochem. 27, 40–46 (in Chinese with English abstract).
Liu, Y.S., Gao, S., Jin, S.Y., Hu, S.H., Sun, M., Zhao, Z.B., Feng, J.L., 2001. Geochemistry of lower crustal xenoliths from Neogene Hannuoba basalt, North China Craton: implications for petrogenesis and lower crustal composition. Geochim. Cosmochim. Acta 65, 2589–2604.
Ma, Q., Zheng, J.P., 2009. In-situ U–Pb dating and Hf isotopic analyses of zircons in the volcanic rock of the Lanqi Formation in the Beipiao area, western Liaoning Province. Acta Petrol. Sin. 25, 3287–3297 (in Chinese with English abstract).
Ma, Q., Zheng, J.P., Griffin, W.L., Zhang, M., Tang, H.Y., Su, Y.P., Ping, X.Q., 2012. Triassic "adakitic" rocks in an extensional setting (North China): melts from the cratonic lower crust. Lithos 149, 159–173.
Martin, H., Smithies, R.H., Rapp, R., Moyen, J.F., Champion, D., 2005. An overview of adakite, tonalite–trondhjemite–granodiorite (TTG), and sanukitoid: relationships and some implications for crustal evolution. Lithos 79, 1–24.
McDonough, W.F., Sun, S.S., 1995. The composition of the Earth. Chem. Geol. 120 (3–4), 223–253.
Menzies, M.A., Fan, W.M., Zhang, M., 1993. Palaeozoic and Cenozoic lithoprobes and the loss of >120 km of Archaean lithosphere, Sino-Korean craton, China. Geol. Soc. (Lond.) Spec. Publ. 76, 71–81.
Moyen, J.F., 2009. High Sr/Y and La/Yb ratios: the meaning of the "adakitic signature". Lithos 112, 556–574.
Pertermann, M., Hirschmann, M.M., 2003. Anhydrous partial melting experiments on MORB-like eclogite: phase relations, phase compositions and mineral-melt partitioning of major elements at 2–3 GPa. J. Petrol. 44 (12), 2173–2201.
Nair, R., Chacko, T., 2008. Role of oceanic plateaus in the initiation of subduction and origin of continental crust. Geology 36, 583–586.
Nehring, F., Foley, S., Hölttä, P., 2010. Trace element partitioning in the granulite facies. Contrib. Mineral. Petrol. 159, 493–519.
Qian, Q., Hermann, J., 2013. Partial melting of lower crust at 10–15 kbar: constraints on adakite and TTG formation. Contrib. Mineral. Petrol. 165, 1195–1224.
Rudnick, R.L., Gao, S., 2003. Composition of the continental crust. In: Rudnick, R.L. (Ed.), Treatise on Geochemistry, vol. 3: The Crust. Elsevier–Pergamon, Oxford, UK, pp. 1–64.
Severs, M.J., Beard, J.S., Fedele, L., Hanchar, J.M., Mutchler, S.R., Bodnar, R.J., 2009. Partitioning behavior of trace elements between dacitic melt and plagioclase, orthopyroxene, and clinopyroxene based on laser ablation ICPMS analysis of silicate melt inclusions. Geochim. Cosmochim. Acta 73, 2123–2141.
Shaw, D.M., 1970. Trace element fractionation during anatexis. Geochim. Cosmochim. Acta 34, 237–243.
Wang, Q., McDermott, F., Xu, J.F., Bellon, H., Zhu, Y.T., 2005. Cenozoic K-rich adakitic volcanic rocks in the Hohxil area, northern Tibet: lower-crustal melting in an intracontinental setting. Geology 33, 465–468.
Wang, Q., Xu, J.F., Jian, P., Bao, Z.W., Zhao, Z.H., Li, C.F., Xiong, X.L., Ma, J.L., 2006a. Petrogenesis of adakitic porphyries in an extensional tectonic setting, Dexing, South China: implications for the genesis of porphyry copper mineralization. J. Petrol. 47, 119–144.
Wang, X.R., Gao, S., Liu, X.M., Yuan, H.L., Hu, Z.C., Zhang, H., Wang, X.C., 2006b. Geochemistry of high-Mg andesites from the early Cretaceous Yixian Formation, western Liaoning: implications for lower crustal delamination and Sr/Y variations. Sci. China, Ser. D, Earth Sci. 49, 904–914.
Xiong, X.L., Adam, J., Green, T.H., 2005. Rutile stability and rutile/melt HFSE partitioning during partial melting of hydrous basalt: implications for TTG genesis. Chem. Geol. 218, 339–359.
Xu, J.F., Shinjo, R., Defant, M.J., Wang, Q., Rapp, R.P., 2002. Origin of Mesozoic adakitic intrusive rocks in the Ningzhen area of east China: partial melting of delaminated lower continental crust? Geology 30, 1111–1114.
Xu, W.L., Wang, Q.H., Wang, D.Y., Guo, J.H., Pei, F.P., 2006. Mesozoic adakitic rocks from the Xuzhou–Suzhou area, eastern China: evidence for partial melting of delaminated lower continental crust. J. Asian Earth Sci. 27, 230–240.
Xu, Y.G., 2001. Thermo-tectonic destruction of the Archaean lithospheric keel beneath the Sino-Korean craton in China: evidence, timing and mechanism. Phys. Chem. Earth, Part A, Solid Earth Geod. 26 (9–10), 747–757.
Yang, W., Li, S.G., 2008. Geochronology and geochemistry of the Mesozoic volcanic rocks in Western Liaoning: implications for lithospheric thinning of the North China Craton. Lithos 102, 88–117.
Zhai, M.G., Guo, J.H., Liu, W.J., 2001. An exposed cross-section of early Precambrian continental lower crust in North China craton. Phys. Chem. Earth, Part A, Solid Earth Geod. 26, 781–792.
Zhang, H.F., Zhu, R.X., Santosh, M., Ying, J.F., Su, B.X., Hu, Y., 2013. Episodic widespread magma underplating beneath the North China Craton in the Phanerozoic: implications for craton destruction. Gondwana Res. 23, 95–107.
Zhang, Q., Wang, Y., Xiong, X.L., Li, C.D., 2008. Adakite and Granite: Challenge and Opportunity. China Land Press, Beijing. (In Chinese with English abstract).
Zheng, J.P., Griffin, W.L., O'Reilly, S.Y., Lu, F.X., Yu, C.M., 2004. U–Pb and Hf-isotope analysis of zircons in mafic xenoliths from Fuxian kimberlites: evolution of the lower crust beneath the North China Craton. Contrib. Mineral. Petrol. 148, 79–103.
Zheng, J.P., Griffin, W.L., O'Reilly, S.Y., Yu, C.M., Zhang, H.F., Pearson, N., Zhang, M., 2007. Mechanism and timing of lithospheric modification and replacement beneath the eastern North China Craton: peridotitic xenoliths from the 100 Ma Fuxin basalts and a regional synthesis. Geochim. Cosmochim. Acta 71 (21), 5203–5225.
Zheng, J.P., Griffin, W.L., Ma, Q., O'Reilly, S.Y., Xiong, Q., Tang, H.Y., Zhao, J.H., Yu, C.M., Su, Y.P., 2012. Accretion and reworking beneath the North China Craton. Lithos 149, 61–78.